Fermilab Library
0 1160 0038675 9

MURA-337-A
Internal

ADDENDUM TO REPORT MURA-337

FIELDS IN SLANTED-GAP EXCITED RECTANGULAR DUCTS

INTRODUCTION

The formulas for energy and momentum kicks given in Report 337 assume that the particles are subjected to essentially D.C. fields upon crossing of the gap region. Such formulas represent the "infinite velocity" limit and, whenever kicks are plotted versus frequency, should yield acceptable results for sufficiently low frequencies only. The following additional data, intended to replace paragraphs 3 and 4 of Report 337, are more rigorous in that they take the finite velocity of the particles into consideration. This gain in generality was fortunately obtained at the expense of very little additional complexity of the formulas.

III. The longitudinal energy kick, for a particle crossing the $Z=0$ plane when the gap voltage is equal to $V\cos\varphi$, turns out to be

$$\Delta\mathcal{E}(X,Y)=q\int_{-\infty}^{+\infty}E_z(X,Y,Z,t)\,dZ=qV_1\cos\varphi+qV_2\sin\varphi$$

with the following expressions for V_1 and V_2 :

$$V_1(X,Y)=-\frac{16V}{\pi^2}\cos\left(tg\theta\frac{\nu}{\beta}\frac{\pi}{2}\right)\sum_{m=1,3}^{\infty}\sum_{n=1,3}^{\infty}\frac{(-1)^{\frac{m+n}{2}}\cos\frac{m\pi X}{a}\cos\frac{n\pi Y}{b}}{m^2+n^2\tau^2+\left(\frac{1}{\beta^2}-1\right)\nu^2}\cdot\frac{m}{n}\cdot\left(1+\frac{n^2\tau^2}{m^2-\left(tg\theta\frac{\nu}{\beta}\right)^2}\right) \qquad (2)$$

$$V_2(X,Y)=-\frac{16V}{\pi^2}\sin\left(tg\theta\frac{\nu}{\beta}\frac{\pi}{2}\right)\sum_{m=0,2}^{\infty}\sum_{n=1,3}^{\infty}\frac{(-1)^{\frac{m+n+1}{2}}\sin\frac{m\pi X}{a}\cos\frac{n\pi Y}{b}}{m^2+n^2\tau^2+\left(\frac{1}{\beta^2}-1\right)\nu^2}\cdot\frac{m}{n}\left(1+\frac{n^2\tau^2}{m^2-\left(tg\theta\frac{\nu}{\beta}\right)^2}\right) \qquad (3)$$

In these expressions, $\nu = f/f_c$ is the frequency measured in terms of the cut-off value, $\beta = v/c$ is the velocity measured in terms of the velocity of light.

The physical significance of the "in phase" voltage V_1 is clear. It is the voltage kick impressed on a particle crossing the $Z=0$ plane when the gap voltage is maximum. The frequency dependence of V_1, for particles moving along the main axis of the guide, is depicted in Figure 6. It will be noticed that the full value of the gap voltage is obtained when the gap is perpendicular to the axis, and the particle travels at the velocity of light. For slanted gaps and lower velocities, the effective gap voltage is reduced by phase effects, even to the point of becoming "decelerating" for certain values of the parameters. This is further illustrated by Figure 7, where the variation of V_1 throughout the cross-section is displayed for a rather extreme set of parameters. The voltage is seen to be decelerating for most

of the points of the cross-section. When the slant angle is reasonably low, however, a more regular behavior is obtained. For a gap perpendicular to the axis, in particular, the effective voltage varies smoothly from the center of the guide, where it is minimum, towards the edges, where its value is equal to V. Still more particularly, the effective voltage is equal to V all through the cross-section for particles traveling at the velocity of light. This interesting result, by the way, is a characteristic property of perpendicular gaps, and is independent of the shape of the duct (rectangular, circular, etc.).[6]

The physical significance of the "quadrature" voltage V_2 is equally clear. It is the voltage impressed on a particle crossing the $Z=0$ plane when the gap voltage is zero, and is becoming negative. It is immediately apparent that V_2 vanishes for a gap perpendicular to the axis, and that its existence can, in consequence, be ascribed to the presence of a slant angle. The frequency dependence of V_2, for particles moving along the center of the narrow wall of the duct, is depicted in Figure 8. The variation of V_2 throughout the cross-section, for an extreme set of parameters, is shown in Figure 9. It will be noticed that, in accordance with equation (3), the quadrature voltage vanishes along the O Y axis. Its variation within the duct is more and more accurately represented by the " δ- function approximation" when (a) the velocity increases, (b) the frequency decreases, (c) the cross-section becomes flatter, (d) the slant angle decreases. The same conclusions are valid for the "in phase" voltage.

IV. The lateral momentum kick is given by the formula

$$\Delta\bar{p}(x,y) = q\int_{-\infty}^{+\infty} \bar{E}_{\text{transv.}}(x,y,z,t)\,dt + q\mu_0 v\int_{-\infty}^{+\infty}\left[\bar{u}_z \times \bar{H}(x,y,z,t)\right]dt = \frac{qV}{c}\bar{p}_1\cos\varphi + \frac{qV}{c}\bar{p}_2\sin\varphi$$

where $\bar{p}_1$, the "in phase" momentum kick expressed in units of qV/c, is equal to

$$\bar{p}_1(x,y) = \frac{16\nu}{\pi^2}\sin\left(tg\,\theta\frac{\nu}{\beta}\frac{\pi}{2}\right)\left\{\bar{u}_x\sum_{m=0,2}^{\infty}\sum_{n=1,3}^{\infty}\frac{(-1)^{\frac{m+n+1}{2}}\cos\frac{m\pi x}{a}\cos\frac{n\pi y}{b}}{\varepsilon_m\, n\left[m^2+n^2\tau^2+\left(\frac{1}{\beta^2}-1\right)\nu^2\right]}\cdot\left[\frac{1}{\beta^2}-1-\frac{n^2\tau^2 tg^2\theta}{m^2-\left(tg\,\theta\frac{\nu}{\beta}\right)^2}\right]\right.$$

$$\left.-\bar{u}_y\tau\left(\frac{1}{\beta^2}+\frac{tg^2\theta}{\beta^2}-1\right)\sum_{m=0,2}^{\infty}\sum_{n=1,3}^{\infty}\frac{(-1)^{\frac{m+n+1}{2}}\cdot m\cdot\sin\frac{m\pi x}{a}\cdot\sin\frac{n\pi y}{b}}{\varepsilon_m\left[m^2+n^2\tau^2+\nu^2\left(\frac{1}{\beta^2}-1\right)\right]\left[m^2-\left(\frac{\nu\, tg\,\theta}{\beta}\right)^2\right]}\right\} \qquad (4)$$

ε_m is Neumann's factor, equal to 2 for m = 0, to 1 for m = 1, 2, 3, . . .

The "quadrature" momentum kick, on the other hand, turns out to be

$$\bar{p}_2(x,y) = \frac{16\nu}{\pi^2}\cos\left(tg\,\theta\frac{\nu}{\beta}\frac{\pi}{2}\right)\left\{\bar{u}_x\sum_{m=1,3}^{\infty}\sum_{n=1,3}^{\infty}\frac{(-1)^{\frac{m+n}{2}}\sin\frac{m\pi x}{a}\cos\frac{n\pi y}{b}}{n\left[m^2+n^2\tau^2+\left(\frac{1}{\beta^2}-1\right)\nu^2\right]}\left[\frac{1}{\beta^2}-1-\frac{n^2\tau^2 tg^2\theta}{\beta^2\left[m^2-\left(tg\,\theta\frac{\nu}{\beta}\right)^2\right]}\right]\right.$$

$$\left.+\bar{u}_y\tau\left(\frac{1}{\beta^2}+\frac{tg^2\theta}{\beta^2}-1\right)\sum_{m=1,3}^{\infty}\sum_{n=1,3}^{\infty}\frac{(-1)^{\frac{m+n}{2}}\cdot m\cdot\cos\frac{m\pi x}{a}\sin\frac{n\pi y}{b}}{\left[m^2+n^2\tau^2+\nu^2\left(\frac{1}{\beta^2}-1\right)\right]\left[m^2-\left(tg\,\theta\frac{\nu}{\beta}\right)^2\right]}\right. \qquad (5)$$

The lateral momentum kick in the center of the guide is of particular interest. Equations (4) and (5) show that it consists of an "in phase" component only, that its direction is parallel to the broad wall of the guide, and that its magnitude decreases the slant angle of the gap. Its frequency dependence is plotted in Figure 10. A conclusion already reached in the analysis of the voltage kick can be confirmed here: the δ- function approximation is good as long as sufficiently high velocities and low frequencies are considered. To emphasize this conclusion still more, the variation of $\bar{p}_1$ throughout a square cross-section is shown in Figure 11 for a rather extreme set of parameters. The actual value of the momentum kick, as given in this figure, is far from the value predicted by the δ- function approximation. The latter value is, in particular, independent of the y coordinate, a result which is not confirmed by the exact analysis.

The δ- function approximation predicts that the lateral momentum kick vanishes for a gap perpendicular to the duct axis. An exact analysis, on the contrary, shows that, because of the presence of magnetic forces, the quadrature momentum kick does not vanish under these conditions. Its frequency dependence, for points located halfway towards the walls on the O X and O Y axes, is depicted in Figure 12. The kick vanishes everywhere for particles traveling at the velocity of light, this in accordance with a very general property established elsewhere.[6] It will be noticed, from Figure 12, that the momentum kick at points located on the O X axis rapidly becomes negligible as the cross-section becomes flatter and flatter. This is not true, however, for points located on the O Y axis, a consideration of importance with the flat "doughnuts" used in the design of the MURA machine. Finally, the variation of the quadrature momentum kick throughout a square cross-section is shown in Figure 13 for a representative set of parameters. There, again, a gap perpendicular to the main axis is considered (space limitations forbid inclusion of more data on slanted gaps).

CONCLUSION

The constancy of voltage phase and amplitude all along the gap contour is not realized with the driving systems commonly encountered in practice (e.g. the single coaxial line driving the gap in one point). The main qualitative results of the present analysis should still remain valid, however. It is found, for instance, that the omission of magnetic field effects, and the assumption of a δ- function behavior for the electric field, yield acceptable results only in the limit of low frequencies and high velocities. Figures 6 to 13 give an idea of the errors introduced by these simplifying assumptions. One result of particular importance was the existence of a lateral momentum kick in circumstances where the δ- function approximation predicted its absence. This fact should be kept in mind when R.F. knockout and betatron oscillations problems are considered.

ACKNOWLEDGMENT

The lengthy calculations supporting the numerical data of this paper have been very ably programmed by Mr. J. McNall on MURA's IBM 704 computer.

Figure 6. "In phase" energy kick as a function of frequency, for X = Y = 0 and (a) $\tau = 1$, (b) $\tau = 5$. For each value of velocity, the three curves refer, starting from the uppermost, to $\theta = 0^{\circ}$, 30°, 60° respectively.

Figure 7. Distribution of the "in phase" energy kick throughout a square cross-section. Parameters: $\theta = 60^{\circ}$, $\nu = 0.5$, $v = \frac{1}{3} c$. Curves labeled in units of qV.

Figure 8. "Quadrature" energy kick as a function of frequency, for X = a/2, Y = 0; and two values of θ. These curves are the same for all values of τ.

Figure 9. Distribution of the "quadrature" energy kick throughout a square cross-section. Parameters: $\theta = 60^{\circ}$, $\nu = 0.5$, $v = \frac{2}{3} c$. Curves labeled in units of qV.

Figure 10. X component of the "in phase" momentum kick along the main axis X = Y = 0, for three velocities and for (a) $\theta = 30^{\circ}$, (b) $\theta = 60^{\circ}$. The three curves of each family correspond, reading down from the uppermost, to $\tau = 1, 2, 5$. The arrows indicate the value predicted by the δ- function approximation.

Figure 11. "In phase" lateral momentum kick for $\theta = 60^{\circ}$, $\nu = 0.5$, $v = \frac{1}{3} c$: the arrow bearing the indication "A" indicates the value which the δ- function approximation predicts for points located on the O Y axis.

Figure 12. "Quadrature" lateral momentum kick for $\theta = 0^{\circ}$, $\nu = 0.5$, $v = \frac{1}{3} c$ and (a) X = a/4 Y = 0, (b) X = 0 Y = b/4. Each aspect ratio is represented by two curves, the upper curve corresponds to $v = \frac{1}{3} c$, the lower curve to $v = \frac{2}{3} c$. The momentum kick for $\tau = 5$, in Figure 12a, is too small to be plotted with accuracy, and has been omitted.

Figure 13. "Quadrature" lateral momentum kick for $\nu = 0.5$, $v = \frac{2}{3} c$ and $\theta = 0^{\circ}$. The particles cross the plane of the gap at the moment the gap voltage goes through zero.

REFERENCES

1. K. R. Symon, D. W. Kerst, L. W. Jones, L. J. Laslett and K. M. Terwilliger, Phys. Rev., 103, 1837 (1956).

2. P. M. Morse and H. Feshback, Methods of Theoretical Physics, (McGraw-Hill Co., New York, 1953) Ch. 13.

3. J. Van Bladel, paper accepted for publication in "Zeitschrift für Angewandte Mathematik und Physik."

4. J. Van Bladel, MURA Internal Report 337, August, 1957.

5. J. Van Bladel, J. Appl. Phys., 28, 1479 (1957).

6. J. Van Bladel, paper accepted for publication in "Nuclear Instruments."

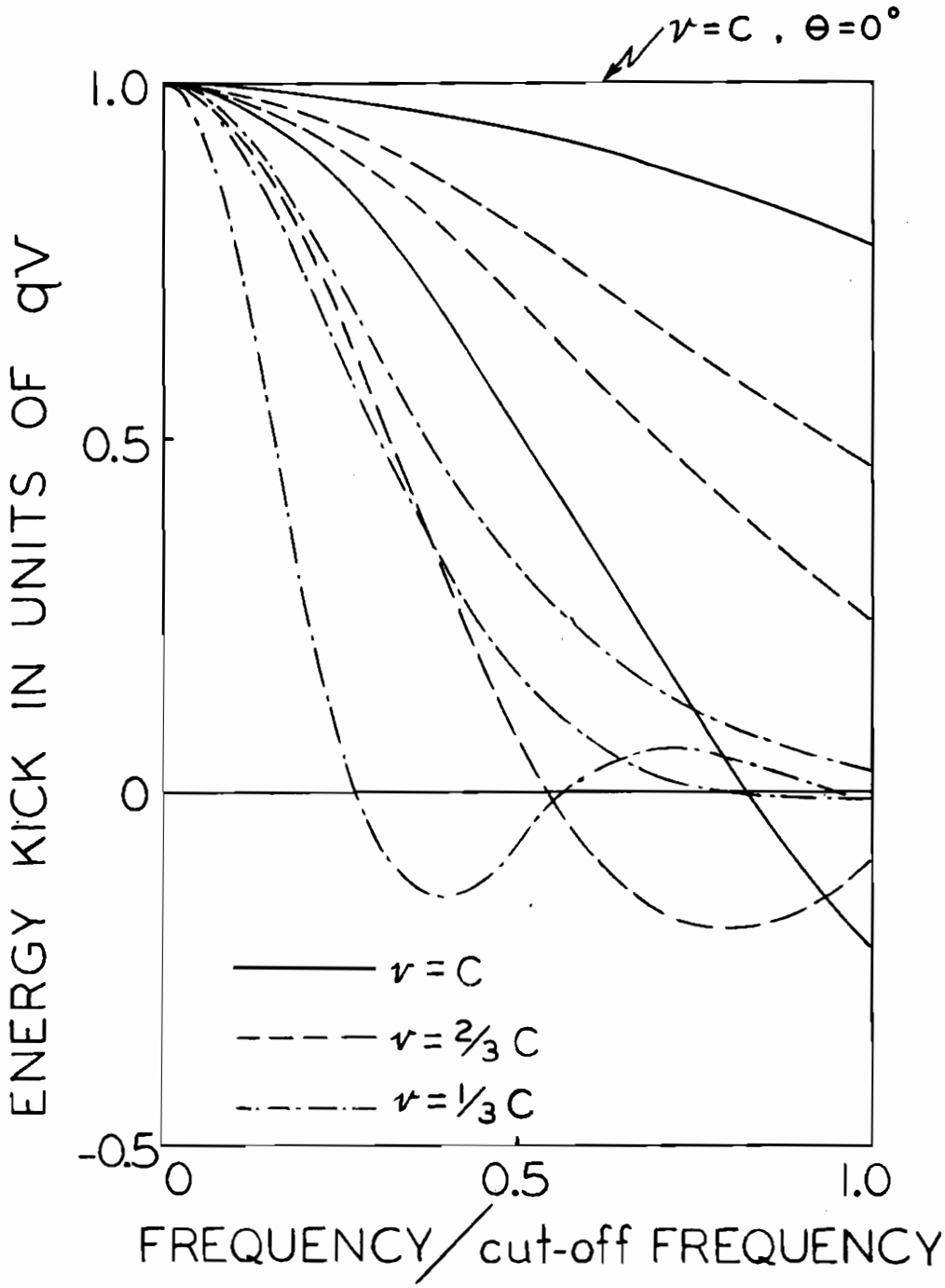
v = C , θ = 0°
1.0
0.5
0
-0.5
ENERGY KICK IN UNITS OF qV
v = C
v = 2/3 C
v = 1/3 C
0
0.5
1.0
FREQUENCY / cut-off FREQUENCY

FIG. 6 (a)

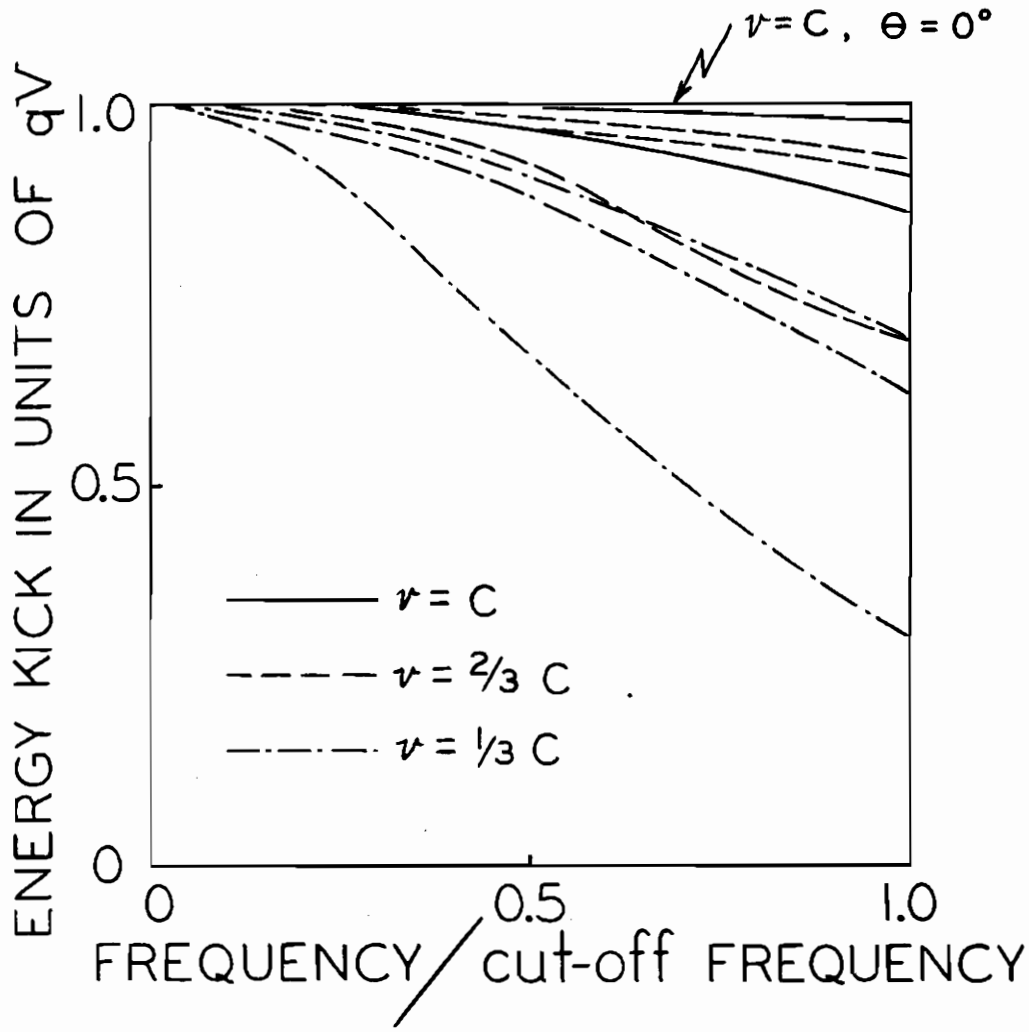
v = C , θ = 0°
ENERGY KICK IN UNITS OF qV
1.0
0.5
0
v = C
v = 2/3 C
v = 1/3 C
0
0.5
1.0
FREQUENCY / cut-off FREQUENCY

FIG. 6 (b)

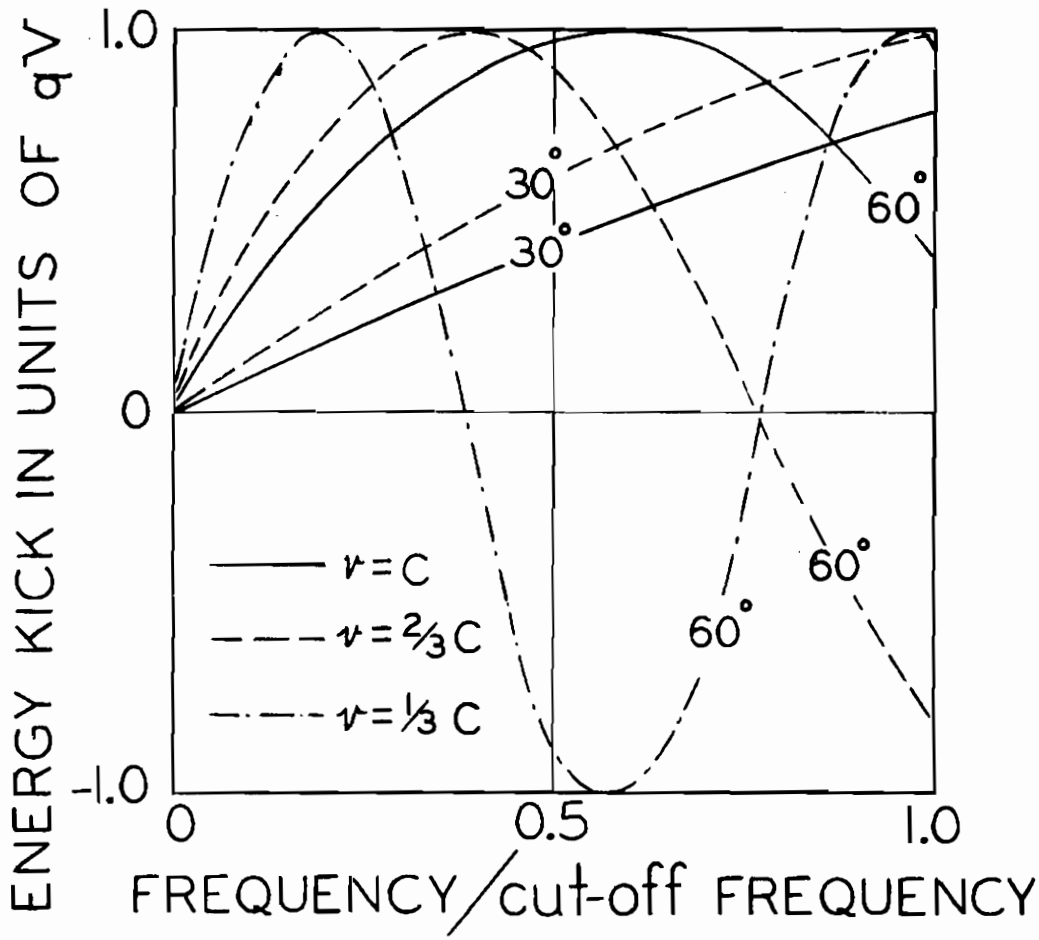
ENERGY KICK IN UNITS OF qV
1.0
0
-1.0
0
0.5
1.0
FREQUENCY/cut-off FREQUENCY
30°
30°
60°
60°
60°
v = C
v = 2/3 C
v = 1/3 C

FIG. 8

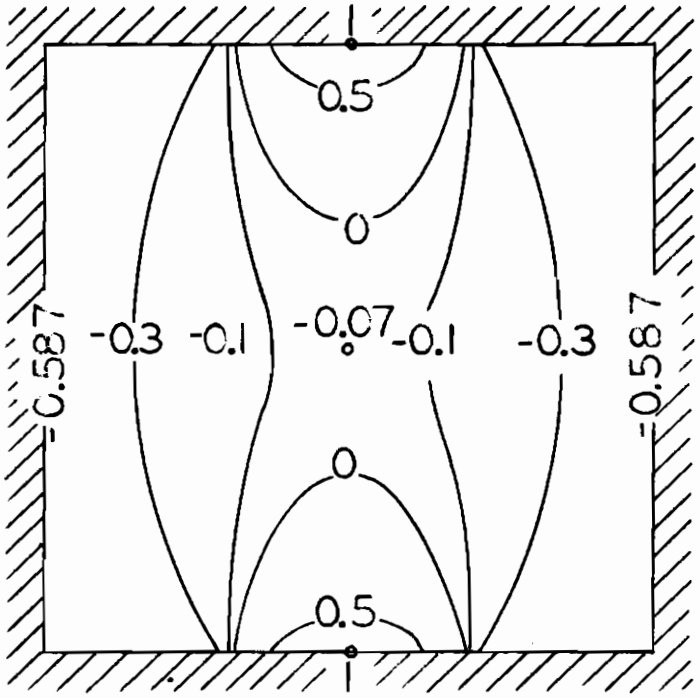
1
0.5
0
-0.587
-0.3
-0.1
-0.07
-0.1
-0.3
-0.587
0
0.5
1

FIG. 7

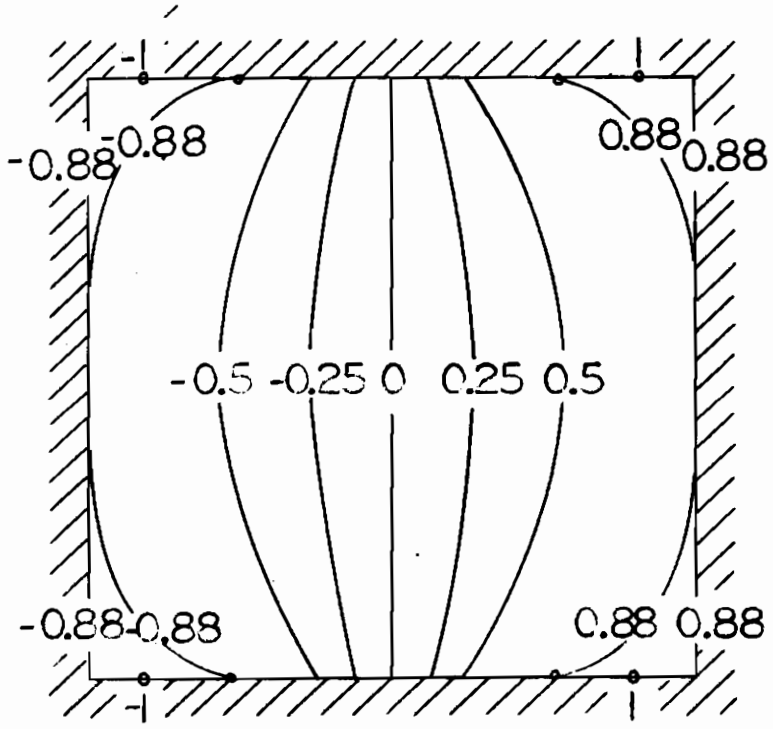
-1
1
-0.88
-0.88
0.88
0.88
-0.5
-0.25
0
0.25
0.5
-0.88
-0.88
0.88
0.88
-1
1

FIG. 9

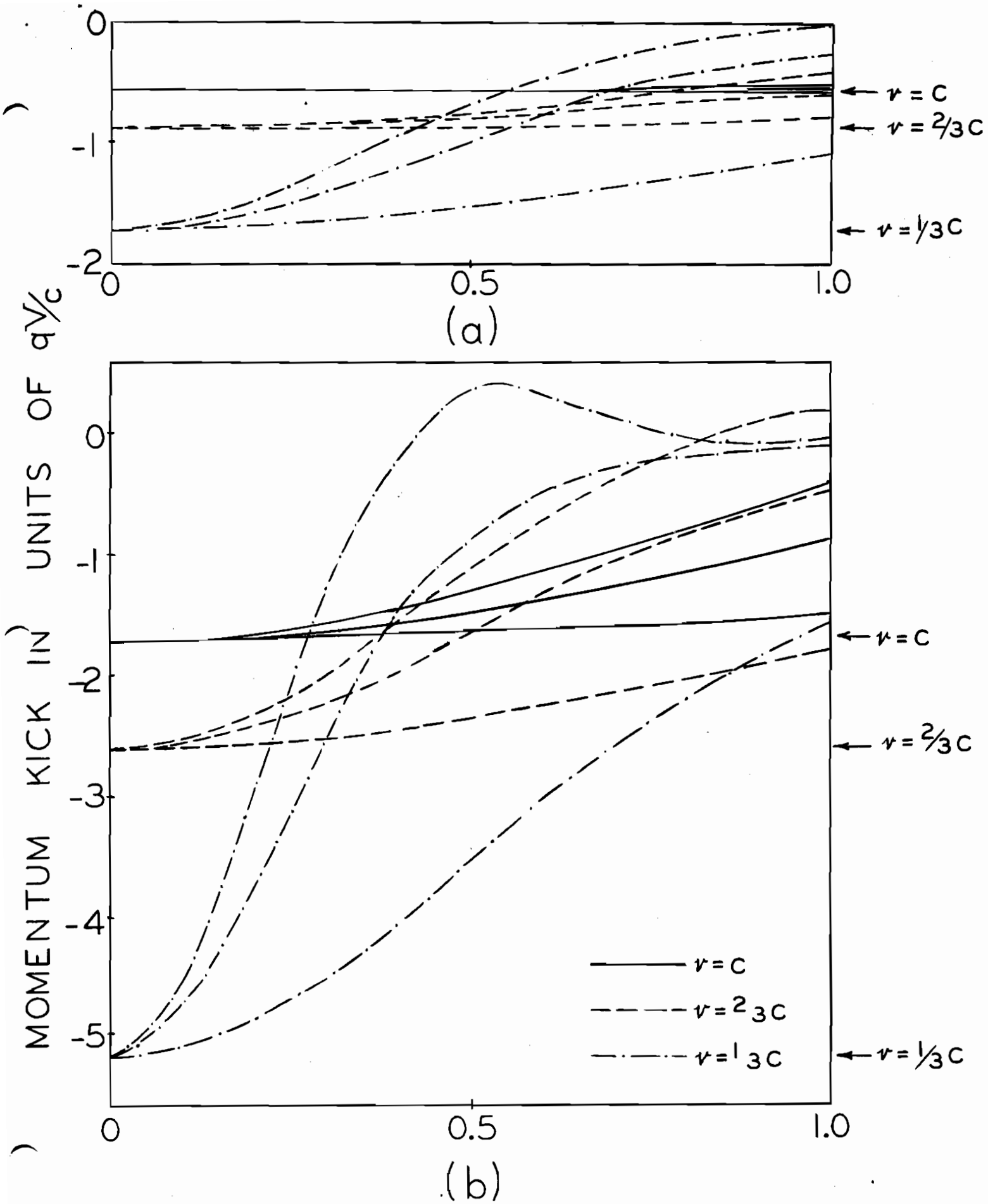
0
-1
-2
0
0.5
1.0
v = c
v = 2/3 c
v = 1/3 c
(a)
MOMENTUM KICK IN UNITS OF qV/c
0
-1
-2
-3
-4
-5
0
0.5
1.0
v = c
v = 2/3 c
v = 1/3 c
v = c
v = 2/3 c
v = 1/3 c
(b)
FREQUENCY/cut-off FREQUENCY

FIG. 10

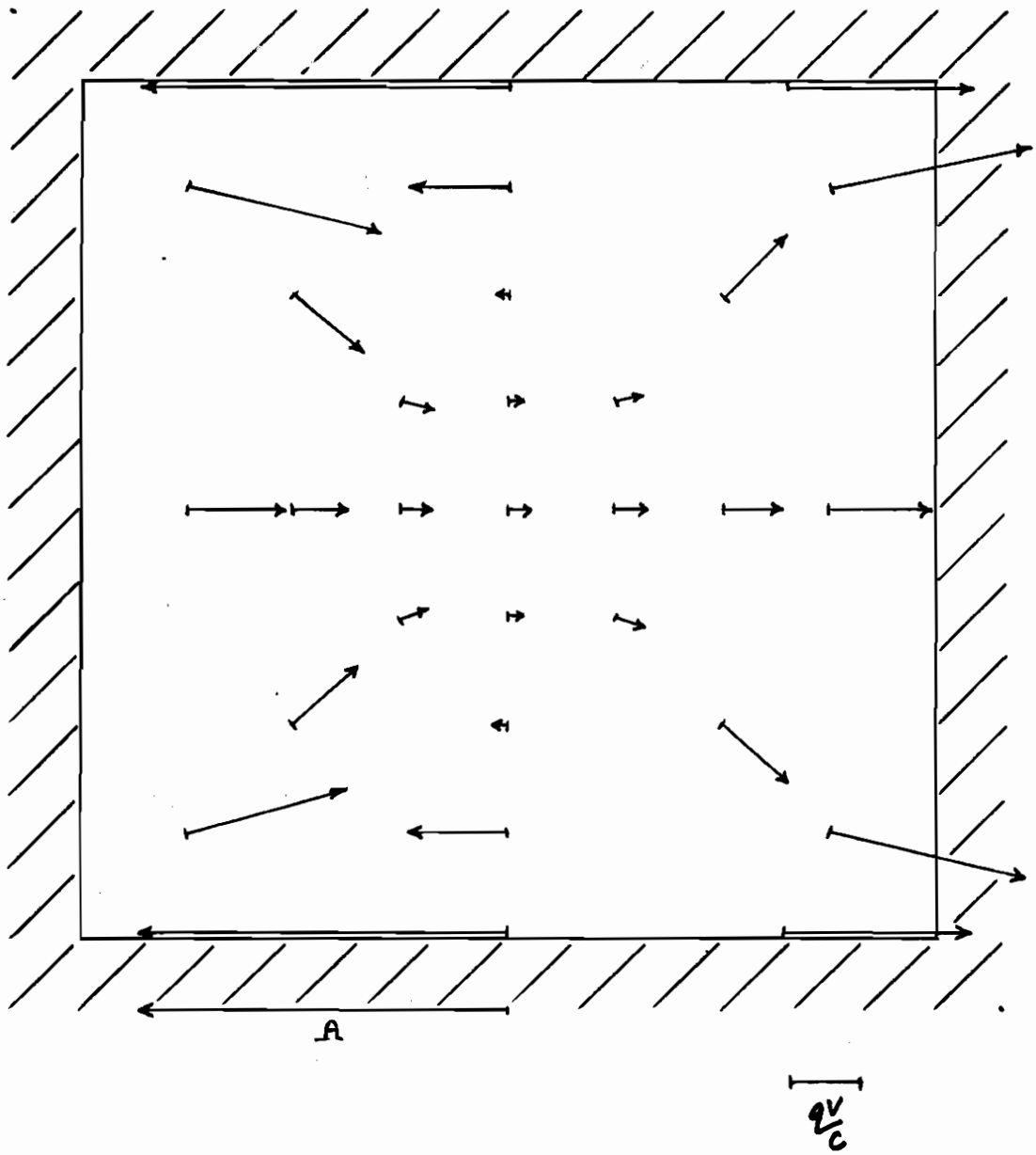

FIG. 11

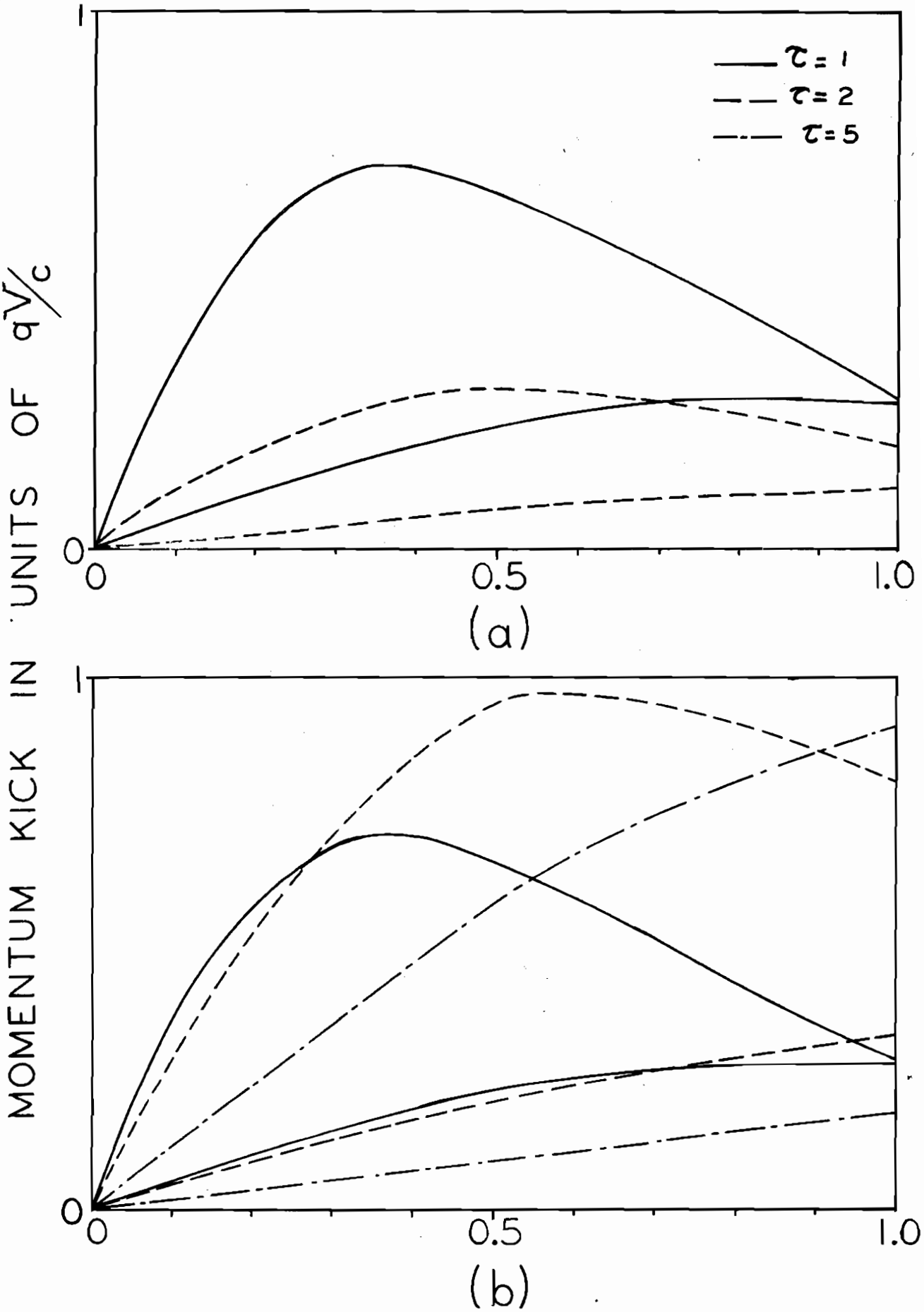
τ = 1
τ = 2
τ = 5
MOMENTUM KICK IN UNITS OF qV/c
1
0
0
0.5
1.0
(a)
1
0
0
0.5
1.0
(b)
FREQUENCY/cut-off FREQUENCY

FIG. 12

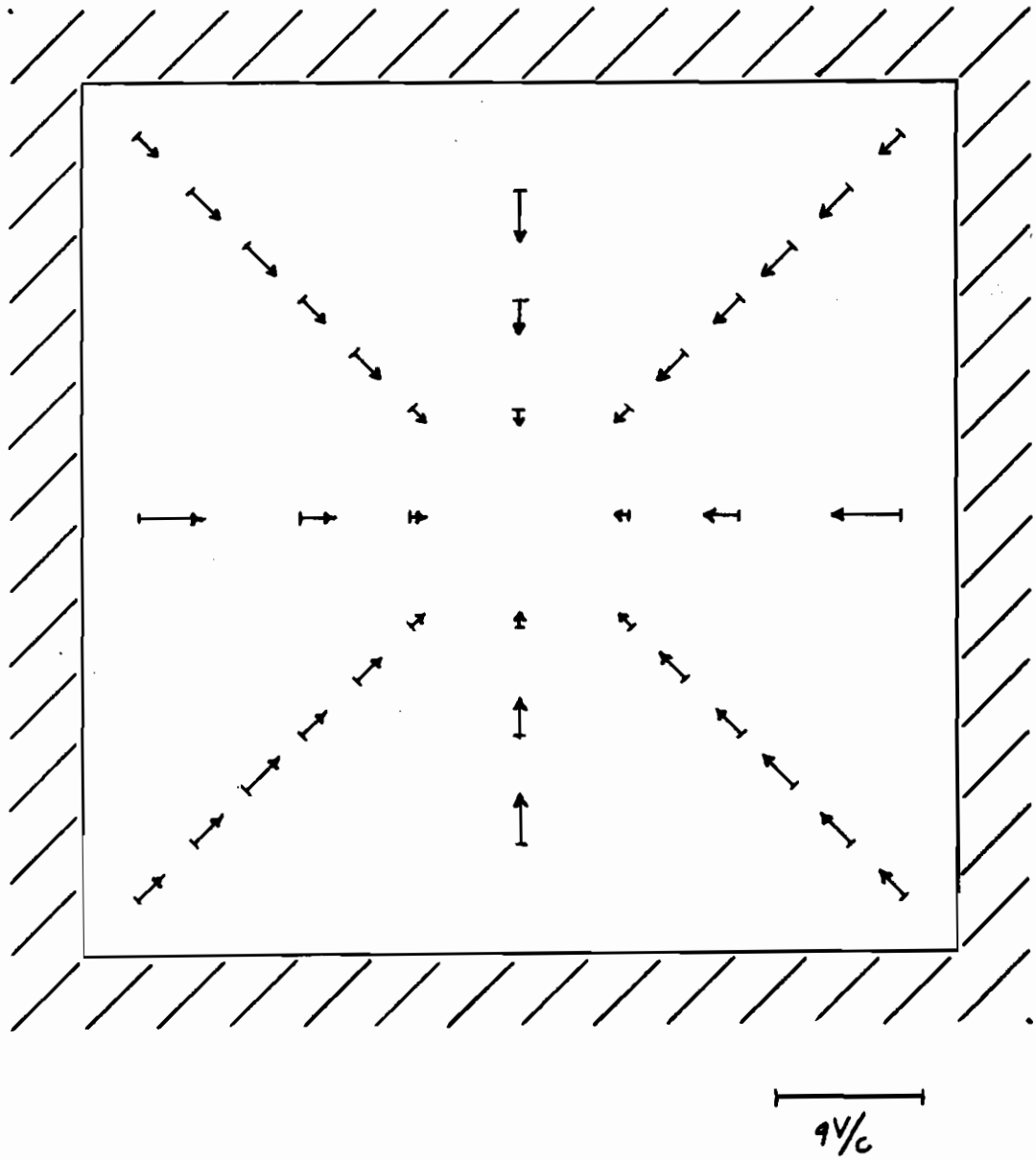

FIG. 13